Simulation of Tearing Mode Suppression Experiments in TEXTOR Based on the Generalized Rutherford Equation

B. Ayten,[1] D. De Lazzari,[1] M.R. De Baar,[1] B.A. Hennen,[1,2] E. Westerhof,[1]
and the TEXTOR Team[3]

[1] *FOM Institute for Plasma Physics 'Rijnhuizen', Association EURATOM-FOM, Trilateral Euregio Cluster, Nieuwegein, Netherlands, www.rijnhuizen.nl*
[2] *Eindhoven University of Technology, Control Systems Technology Group, PO Box 513, 5600 MB Eindhoven, the Netherlands*
[3] *Institute for Energy Research – Plasma Physics, Forschungszentrum Jülich GmbH, Association EURATOM-FZJ, Trilateral Euregio Cluster, 52425 Jülich, Germany*

E-mail: *b.ayten@rijnhuizen.nl*

Introduction

Control of neoclassical tearing modes (NTMs) is of great importance to achieve high performance tokamak discharges as required for nuclear fusion [1]. Both electron cyclotron current drive (ECCD) and electron cyclotron resonance heating (ECRH) localized at the island position are widely used to suppress NTMs [2]. NTM control will also be one of the main tasks of the ITER ECRH system [3]. Projections of the requirements in terms of power and localization of the ECCD are based on the generalized Rutherford equation (GRE), which describes the nonlinear evolution of tearing modes [1]. Experimental benchmarks of the predictions of the GRE are thus highly desirable to strengthen the basis of these projections. So far, most work has been focused on the localized current drive term in the GRE [1,4]. However, in present day experiments the stabilizing contribution from localized heating cannot be neglected [5] and should be accounted for when extrapolating to ITER. Here we provide a benchmark of the heating term in the GRE by focusing on experiments performed on the TEXTOR tokamak, in which the suppression of $m/n = 2/1$ magnetic islands was shown to be dominated by the effect of localized heating [6, 7].

The generalized Rutherford equation

The nonlinear evolution of the full width w of the magnetic island from a neoclassical tearing mode with poloidal and toroidal mode numbers m and n at the resonant radius r_s is described by the generalized Rutherford equation (GRE), which can symbolically be written as

$$0.82\frac{\tau_r}{r_s}\frac{dw}{dt} = r_s\Delta'_0 + r_s\Delta'_{bs} - r_s\Delta'_{pol} + r_s\Delta'_{RMP} - r_s\Delta'_H - r_s\Delta'_{CD}\,. \quad (1)$$

Here, $\tau_r \equiv \mu_0 r_s^2/\eta$ is the resistive diffusion time scale, and the different terms on the right hand side represent different driving and stabilizing mechanisms. In particular, Δ'_0 is the classical tearing mode stability index, Δ'_{bs} represents the neoclassical drive from the annihilation of the bootstrap current inside a finite size island, and Δ'_{pol} the effect of the ion polarization current. In case of the low β TEXTOR experiments, these latter two terms may be neglected. Next, $r_s\Delta'_{RMP} = 2m(w_{vac}/w)^2$ represents the effect from resonant magnetic perturbations (RMP) as applied from the TEXTOR Dynamic Ergodic Diverter (DED). Under the conditions of the experiments, the vacuum fields from the DED would result in an island size w_{vac} = 4 cm. The stabilizing effects from heating and current drive are in accordance with Ref. [5] written as

$$r_s\Delta'_{H,CD} = \frac{16\mu_0 L_q P_{tot}}{B_p \pi w_{dep}^2}\eta_{H,CD} F_{H,CD}(w/w_{dep}, r_{dep} - r_s, M)\,, \tag{2}$$

where $L_q \equiv q/(dq/dr)$ is the magnetic shear length, P_{tot} the total heating or current drive power, B_p the poloidal magnetic field, w_{dep} the full width of the power deposition profile, $\eta_{H,CD} \equiv I/P$ the efficiency of current generation from either heating or direct current drive, and the $F_{H,CD}$ are normalized geometric functions depending on the relative island size, location of power deposition and power modulation (symbolically indicated by M). The 'inductively generated current' from the temperature perturbation caused by the localized heating is estimated as [5]

$$\eta_H = \frac{3w_{dep}^2}{8\pi R n_e \chi_\perp k_B}\frac{j_{sep}}{T_{sep}}\,, \tag{3}$$

where j_{sep} and T_{sep} are the inductive current density and temperature at the island separatrix, R the major radius, and $\chi_\perp$ is the perpendicular electron heat conductivity inside the island.

Experimental set-up and data interpretation

A 12 cm wide 2/1 island was created by the DED (operated in 3/1 mode at 1 kHz AC with a maximum current of 2 kA) in a standard TEXTOR discharge (B_ϕ = 2.25 T, I_p = 300 kA, line averaged density $2 \times 10^{19}\,\mathrm{m}^{-3}$) and suppressed by ECRH/ECCD [6,7]. The location of the 140 GHz ECRH was varied by changing the poloidal injection angle. Different levels of continuous and modulated power were applied. Current drive was affected by varying the toroidal injection angle. The suppression of the island size is estimated from the suppression of 1 kHz temperature oscillations, ΔT_{ECE}, in an ECE channel (141 GHz) coming from near the magnetic island. Rather than the linear dependence assumed in Ref. [6], the island size is estimated as $w \propto \sqrt{\Delta T_{ECE}}$. This square root dependence follows from the observation that $w \propto \sqrt{\psi}$, i.e. the square root of the perturbed flux, while outside the island the temperature perturbation scales linearly with ψ. It is also consistent with independent measurements of the island suppression rate from soft x-rays [6] or ECE-imaging [7] as shown in Fig. 1.

Parameter choices and results of simulations

The parameters for the simulations are chosen in accordance with Ref. [6,7]. This means that the classical tearing mode stability index is approximated with $\Delta'_0(w) = -117\ w + 12\ [m^{-1}]$, the current density and temperature at the separatrix are $j_{sep} = 6.5 \times 10^2$ kA/m^2 and $T_{sep} = 0.5$ keV, respectively, and the perpendicular heat conductivity is $\chi_\perp = 1.2$ m^2/s. The location of the power deposition, the power deposition profile width and the driven current are obtained from beam tracing calculations using the TORBEAM code [8].

The suppression rate is defined as the ratio of the saturated island size during the ECRH/ECCD phase, w_{ECRH}, over the saturated island size as driven by the DED without ECRH, w_{DED}. Figures 2, and 3 show the simulated suppression rate for two experimental scans selected from Ref. [6], namely, a deposition scan with quasi-perpendicular injection of the ECRH, and a scan of the phase of modulated power with a 50% duty cycle, respectively. The experimental suppression rates are given for comparison. Figure 4 shows a comparison of the simulated and measured suppression rates from all discharges discussed in Ref. [6] including in addition to data from Figs. 2 and 3, data from a deposition scan with oblique injection, a modulated power duty cycle scan, and a driven current scan.

Conclusion and Discussion

The simulated suppression rates are in reasonable agreement with the measured suppression rates, thus providing an experimental confirmation of the heating term in the generalized Rutherford equation. However some notable differences between simulations and experiments can be seen. In particular, the experimental data from the deposition scan suggest that additional effects (not included in the present model) should play a role for deposition away from r_s, leading to destabilization for heating inside and additional stabilization for heating outside r_s. In addition the simulations appear to slightly overestimate the suppression as can be seen from the overview presented in Fig. 4. Sensitivity of these results to the assumed parameters, in particular $\chi_\perp$ and $r_{dep} - r_s$, is under investigation.

Acknowledment This work, supported by the European Communities under the contract of association between EURATOM/FOM, was carried out within the framework of the European Fusion programme. The views and opinions expressed herein do not necessarily reflect those of the European Commission. The work forms part of the NWO-RFBR Centre of Excellence Nr. 047.018.002 on Fusion Physics and Technology.

[1] R.J. La Haye, Phys. Plasmas **13** (2006) 055501.
[2] R. Prater, Phys. Plasmas **11** (2004) 2349.
[3] M.A. Henderson, et al., Nucl. Fusion **48** (2008) 054013.
[4] L. Urso, et al., Plasma Phys. Control. Fusion 52 055012
[5] D. De Lazzari, E. Westerhof, Nuclear Fusion **49** (2009) 075002.
[6] E. Westerhof et al., Nuclear Fusion **47** (2007) 85.
[7] I.G.J. Classen et al., Physical Review Letters **98** (2007) 035001.
[8] E. Poli, et al., Comp. Phys. Communications **136** (2001) 90.

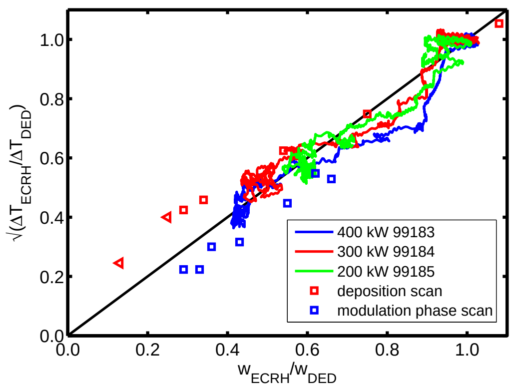

Figure 1. A comparison of the suppression rate, $w_{\mathrm{ECRH}}/w_{\mathrm{DED}}$ with the square root of the normalized temperature oscillation. The full lines shown are obtained by comparing with the relative island width as obtained from ECE-imaging in Ref. [7] as the island evolves from its original size to its suppressed size during the ECRH phase. The symbols show a comparison with suppression rates estimated from SXR data [6] from the deposition and the modulation phase scans shown in Fig. 2 and 3, respectively.

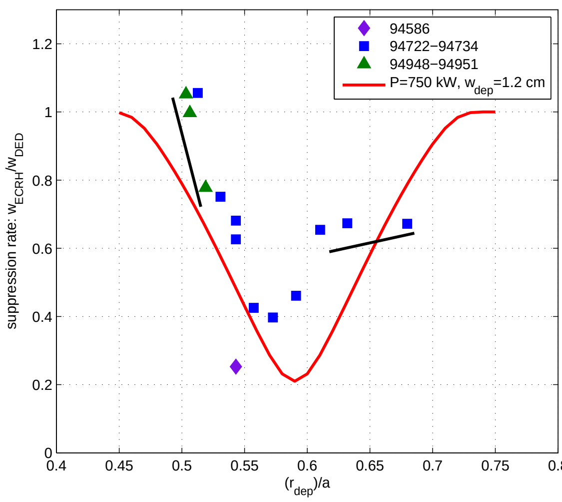

Figure 2. The suppression rate as a function of the deposition location, r_{dep}. The full line shows the result from the simulations with the GRE assuming the q=2 surface is located at r_s/a = 0.59. The symbols show the suppression rate as obtained from the square root of the normalized temperature oscillations observed on the 141 GHz ECE channel. Different symbols refer to discharges from different experimental days.

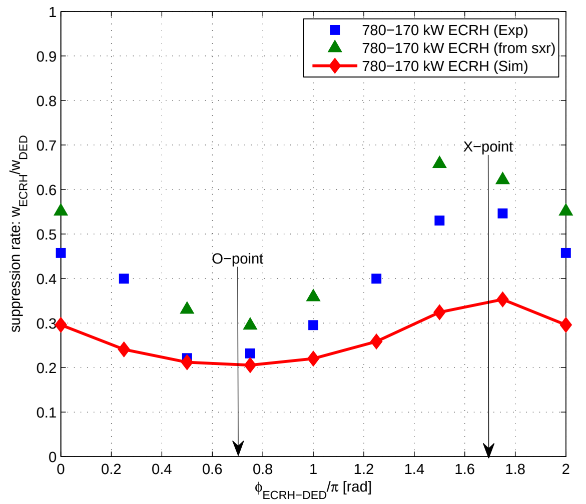

Figure 3. The suppression rate as a function of the modulation phase in case of power modulation with a duty cycle of 50%. The full line represents the results from the simulations and the symbols indicate the suppression rate as estimated from the square root of the observed temperature oscillations in the 141 GHz ECE channel. The modulation phase is given relative to the phase of the DED current (used as reference signal in the experiments). The arrows indicate the estimated positions of the O- and X-point.

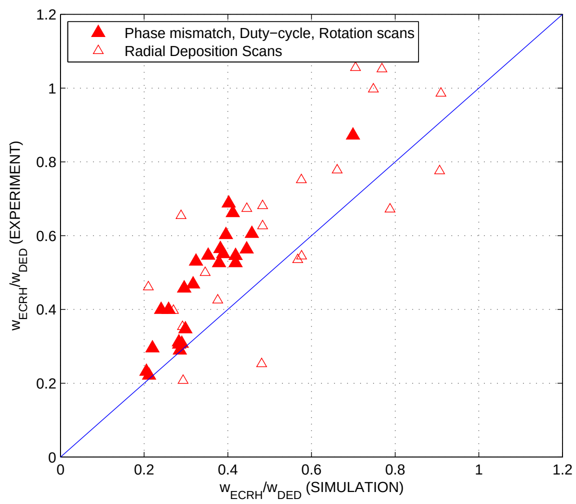

Figure 4. Comparison of the simulated suppression rate with the experimentally estimated suppression rate. Each symbol shows the result from an individual discharge. The different scans refer to the respective figures from Ref. [6] on which the experimental estimates are based.